Inclination and heterogeneity of layered geological sequences influence dike-induced ground deformation

Matías Clunes[1], John Browning[1,2,3*], Carlos Marquardt[1,3], Jorge Cortez[1], Kyriaki Drymoni[4], and Janine Kavanagh[5]

[1]*Department of Structural and Geotechnical Engineering, Pontificia Universidad Católica de Chile, Santiago, Chile*

[2]*Andean Geothermal Centre of Excellence (CEGA), Universidad de Chile, Santiago, Chile*

[3]*Department of Mining Engineering, Pontificia Universidad Católica de Chile, Santiago, Chile*

[4]*Department of Earth and Environmental Sciences, Università degli Studi di Milano-Bicocca, Milan, Italy*

[5]*School of Environmental Sciences, University of Liverpool, Liverpool, United Kingdom*

* *jbrowning@ing.puc.cl*

ABSTRACT

Constraints on the amount and pattern of ground deformation induced by dike emplacement are important for assessing potential eruptions. The vast majority of ground deformation inversions made for volcano monitoring during volcanic unrest assume that dikes are emplaced in either an elastic-half space (a homogeneous crust) or a crust made of horizontal layers with different mechanical properties. Here, we extend these models by designing a novel set of two-dimensional Finite Element Method numerical simulations that consider dike induced surface deformations related to a mechanically heterogeneous crust with inclined layers, thus modelling a common geometry in stratovolcanoes and crustal segments

that have been folded by tectonic forces. Our results confirm that layer inclination can produce localized ground deformations which may be up to 30 times higher in terms of deformation magnitude than would be expected in a purely homogeneous model, depending on the angle of inclination and the stiffness of the rock units that host and are close to the dike, generating asymmetrical deformation patterns with peaks located as much as 1.4 km away from the expected in the homogeneous model. These results highlight the necessity to accurately quantify both the mechanical properties and attitude of the geology underlying active volcanoes.

Keywords: Magmatic intrusion, inclined layers, surface deformation, volcano deformation, volcano heterogeneity

INTRODUCTION

Volcanic eruptions can occur when a magma-filled fracture (a dike if it is vertical, a sill if horizontal, or an inclined sheet if it is neither vertical nor horizontal) propagates from a magma source through the crust up to the surface (Gudmundsson et al., 1999; Rivalta et al., 2015, Acocella, 2021). The emplacement of the magma deforms the crust which may result in ground deformation signals that can be measured and used to infer information about the intrusion such as depth, volume, shape and orientation which may be useful for determining potential eruption characteristics (Geshi et al., 2020). However, the vast majority of models used in volcano monitoring to infer the deformation associated with magmatic emplacement assume that the crust is either isotropic (an elastic half-space) (Okada, 1985), or mechanically stratified with horizontal layers (Masterlark, 2007; Bazargan and Gudmundsson, 2019; 2020). Both assumptions are likely gross simplifications, especially in areas where volcanoes

are built atop highly folded and deformed rocks, such as in Cordillera settings (Clunes et al., 2021). In addition to inclined layers underlying a volcano, the slopes of the upper parts of many stratovolcanoes are inclined by as much as 40°. In both situations it is not reasonable to assume that dikes propagate through horizontal layers. It is also now well known that rock layers that constitute a volcano may vary considerably in terms of their mechanical properties (Drymoni et al., 2020; Heap et al., 2020; Kendrick et al., 2021; Maccaferri et al., 2010). Given these observations, it is perhaps likely that most dikes are emplaced in heterogeneous crustal segments with layers that are somewhat inclined, even in extensional environments albeit the layer inclination may be minor (i.e., <10°) (e.g., Gudmundsson, 1983). Therefore, it is necessary to constrain the deformation signals associated with both heterogeneous and inclined layered sequences and compare the differences associated with commonly used simplified crustal assumptions.

There have been several attempts to constrain crustal deformation in heterogenous layered sequences through numerical modelling (i.e., Gudmundsson, 2002; Gudmundsson and Philipp, 2006; Manconi et al., 2007; and Masterlark, 2007). Masterlark (2007) demonstrated using a combination of analytical and finite element models that the widely used Mogi (1958) model, which considers a point-pressure source embedded in a homogeneous, isotropic segment, can generate substantial displacement prediction errors and significantly inaccurate deformation source parameters if the crustal unit is heterogenous. In that work, the presence of weak layers in a caldera resulted in a deformation source located more than 1000 m deeper. Bazargan and Gudmundsson (2019; 2020), analyzed both the stresses and displacements generated at the surface by magmatic intrusions in horizontally layered rocks. They showed that the presence of compliant layers (with low Young's modulus) increases the surface

deformation expressed during dike or inclined sheet emplacement, and that intrusions meeting layered sequences at lower angles the generates larger surface displacements.

Although significant progress has been made in volcano monitoring in the past decades (Sparks et al., 2012) we still cannot yet forecast with any certainty when and where a magmatic dike will emplace or erupt and this becomes further complicated in highly deformed crustal settings such as the Andes where the host rock is commonly formed by rock layers inclined at different angles, in part because understanding of the role of crustal properties and geometry through which the dikes propagate is lacking. Here we present a series of novel 2D numerical models using the Finite Element Method (FEM) that consider dike-induced ground deformation resulting from a crustal segment hosting contrasting mechanical properties and with variably dipping layers.

NUMERICAL MODEL SETUP

The FEM software COMSOL Multiphysics 5.4 was used to analyze dike-induced surface displacements in a layered crustal segment comprising either horizontal or inclined layers (Figure 1A and 1B). The dimensions of the layered crustal segment hosting the dike were 20 km wide x 20 km deep[1], tested as being sufficient to avoid boundary effects. The dike was modeled as an elliptical cavity of 1 m thickness and its geometry and location in the model domain was varied by changing the dike length and emplacement depth (1, 2 and 4 km).

The crustal segment hosting the dike was modeled as a linear-elastic solid since the primary interest was on the influence of elastic properties on ground deformation. The inclined layers, with contrasting elastic properties (Young's modulus ratios)[2], were made to dip by 10, 25 and 45°. Both the upper and lower layers were assigned alternating Young's modulus of either 1, 10 or 100 GPa such that four stiffness ratios were examined between the different models, 100:1, 10:1, 1:10, 1:100, where the first number relates to the layer hosting the dike (E_1) and the second to the layer above the dike (E_2). To compare our results with the more common modeling protocol we also tested a horizontally layered sequence using contrasting elastic properties and a homogeneous crustal segment with only one Young's modulus of 50 GPa. The only boundary load in the model comes from an internal magmatic overpressure (P_o) of 5 MPa. The upper boundary of the model is a free surface, and it is along this surface that the horizontal and vertical displacements were measured. The other boundaries of themodel are fixed, indicated by crosses, so as to avoid rigid-body translation and rotation. The dipping layers are always located in the right-side of the crustal segment.

[1]A comparison between vertical and horizontal ground deformations obtained from different domain sizes is provided in the Supplemental Material (Figures S1 and S2).
[2]An extended explanation about the numerical modeling setup is provided in the Supplemental Material.

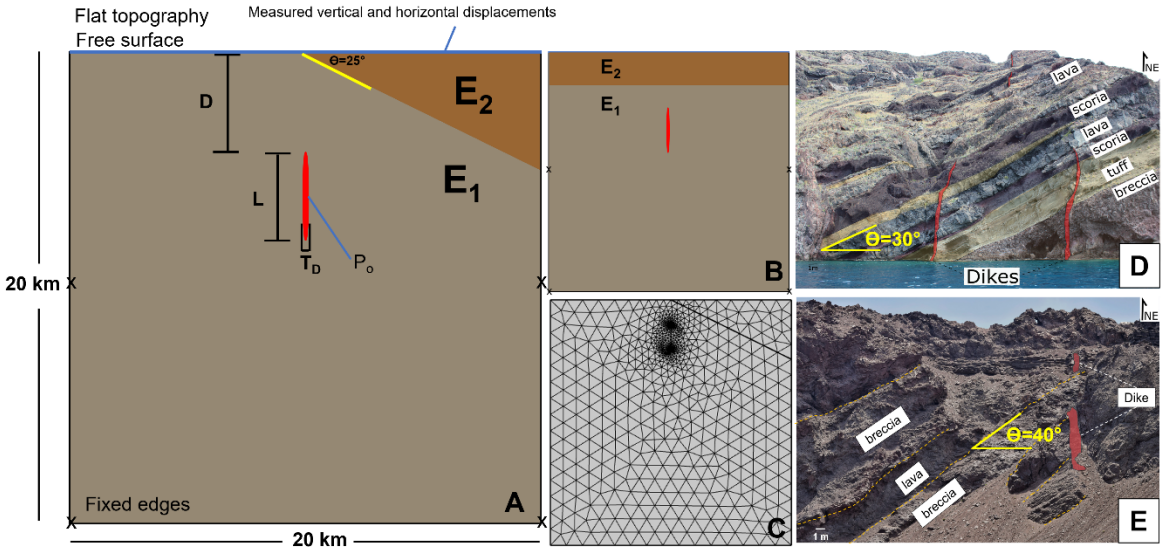

Figure 1: A) FEM model setup for the various layer inclinations tested (L: dike length, T_D: dike thickness, D: upper dike tip depth, P_o: magmatic overpressure, Θ: layer inclination, E_1-E_2: alternating Young's modulus). B) Horizontally mechanical layered model setup C) Example of the model mesh with layers inclined at 25°. D) and E) Field photographs of dikes emplaced in variably dipping rock units from Santorini volcano (Greece) and the Andes (Chile), respectively[3].

VERTICAL GROUND DISPLACEMENTS

Figure 2 demonstrates horizontal profiles along the upper free surface where vertical deformation induced by a 2 km length dike which its upper tip is emplaced at 2 km depth[4]. In both the homogenous and horizontally layered models, the vertical ground deformation is

[3]The locations of both case study are located in the Supplemental Material (Figure S3).
[4]Models that consider other dike lengths and emplacement depths are given in the Supplemental Material in Figures S4-S19.

symmetrically distributed and peaks between around 2.4 and 4.8 km on either side of the dike. The vertical ground deformation becomes asymmetrically distributed when the inclined layers are modeled, and its magnitude is consistently larger as the Young's modulus ratio decreased. The vertical displacements above the inclined layer (to the right of the dike) are greater than calculated above the homogenous segment (to the left of the dike) when the layer hosting the dike is stiffer than the inclined layer (Figures 2A and 2C). Conversely, when the layer hosting the dike is more compliant than the inclined layer, the vertical deformation is greater above the homogeneous segment (Figures 2B and 2D). In this case, when the inclined layer is stiff, the asymmetric deformation is more pronounced when the stiffness contrast is greatest (i.e., 1:100 rather than 1:10). In this case the maximum peak offset is located 1.4 km away from the homogeneous model for an inclination of 45°. However, the opposite is found when the layer above the dike is compliant such that the larger stiffness contrast (100:1) demonstrates a more symmetrical deformation pattern than the lower stiffness contrast (10:1). When the inclined layer is compliant, the amount of vertical ground deformation increases with layer inclination. For example, in the 10:1 case (Figure 2C) for the inclined layer dipping at 45º the maximum vertical displacement is 19 cm, at 25º is 16.3 cm, and at 10º is 13.5 cm. The opposite pattern is observed when the inclined layer is stiff, such that the amount of vertical surface deformation decreases with layer inclination. For example, in the 1:10 case with the layer dipping at 10º the maximum vertical displacement is 82 cm, at 25º is 52 cm and at 45º is 30 cm. When the Young's modulus of the inclined layer is higher than that of the layer hosting the dike, we observed that the vertical deformation when the layer is inclined at 10° is less than that the observed when the layer is horizontal. Oppositely, when the Young's modulus of the layer above the dike is lower than the layer hosting the dike, the

deformation recorded when the layer is inclined at 10° is greater than observed when the layer is horizontal.

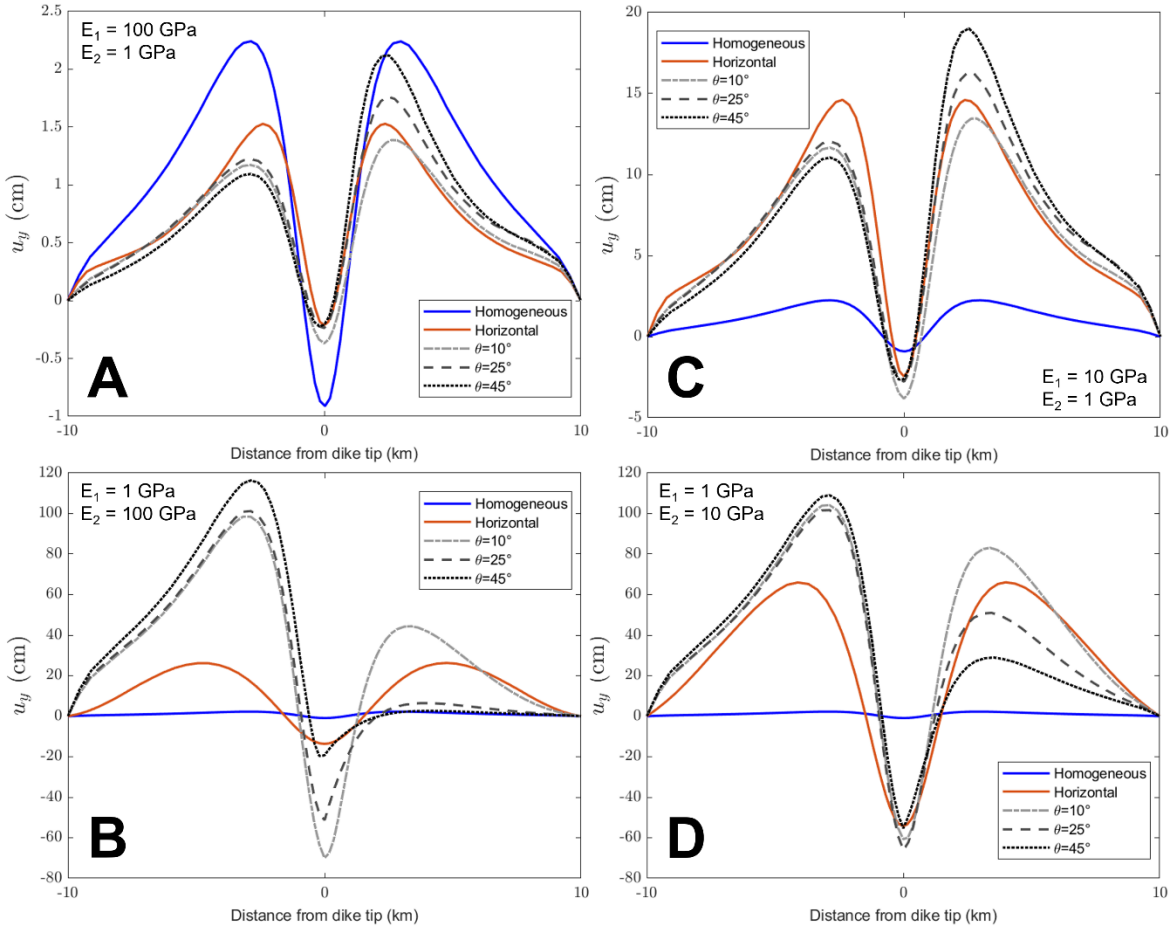

Figure 2: Vertical ground displacement (u_y) variations relative to the lateral distance from the dike tip for each layer inclination and stiffness contrasts tested.

HORIZONTAL GROUND DISPLACEMENTS

Figure 3 reports horizontal profiles of horizontal deformation along the upper surface of the model domain for the Young's modulus ratios tested where the position of the center of the dike is again marked at zero. In both homogeneous and horizontally layered models the horizontal ground deformation is symmetrically distributed and peaks between 4.4 and 7 km on either side of the dike. In these results, the component of horizontal deformation is oriented with respect to the center of deformation above the dike, such that negative

horizontal deformation simply represents ground movement in the opposite direction with respect to the positive values. In all cases the overall deformation signal is extensional, such that each side of the model domain above the dike move away from one another, as expected during dike emplacement. However, when the modeled layers are inclined, the amount of horizontal deformation is different above the area with the inclined layer than the area without the layer such that the extension is asymmetric. This effect is most pronounced when the inclined layer is stiffer than the layer hosting the dike (Figure 3B and D). In this case the maximum peak offset is located 2.4 km away from the horizontally layered model for an inclination of 10° and 1.1 km away from the homogeneous model for an inclination of 45°. When the inclined layer is compliant, the amount of horizontal ground deformation recorded over the inclined layer increases with layer inclination. For example, in the 10:1 case (Figure 3C) with the layer dipping at 45° the maximum horizontal displacement is 29.1 cm, at 25° is 25.1 cm and at 10° is 19.9 cm. As observed for vertical ground deformation, the amount of horizontal surface deformation recorded over the inclined layer decreases with layer inclination when the layer above the dike is stiff. This effect is more pronounced when the stiffness ratio is 1:10 as observed in Figure 3D. In this case the maximum horizontal deformation with the layer dipping at 10º is 42.2 cm, at 25º is 34.6 cm and at 45º is 25.6 cm.

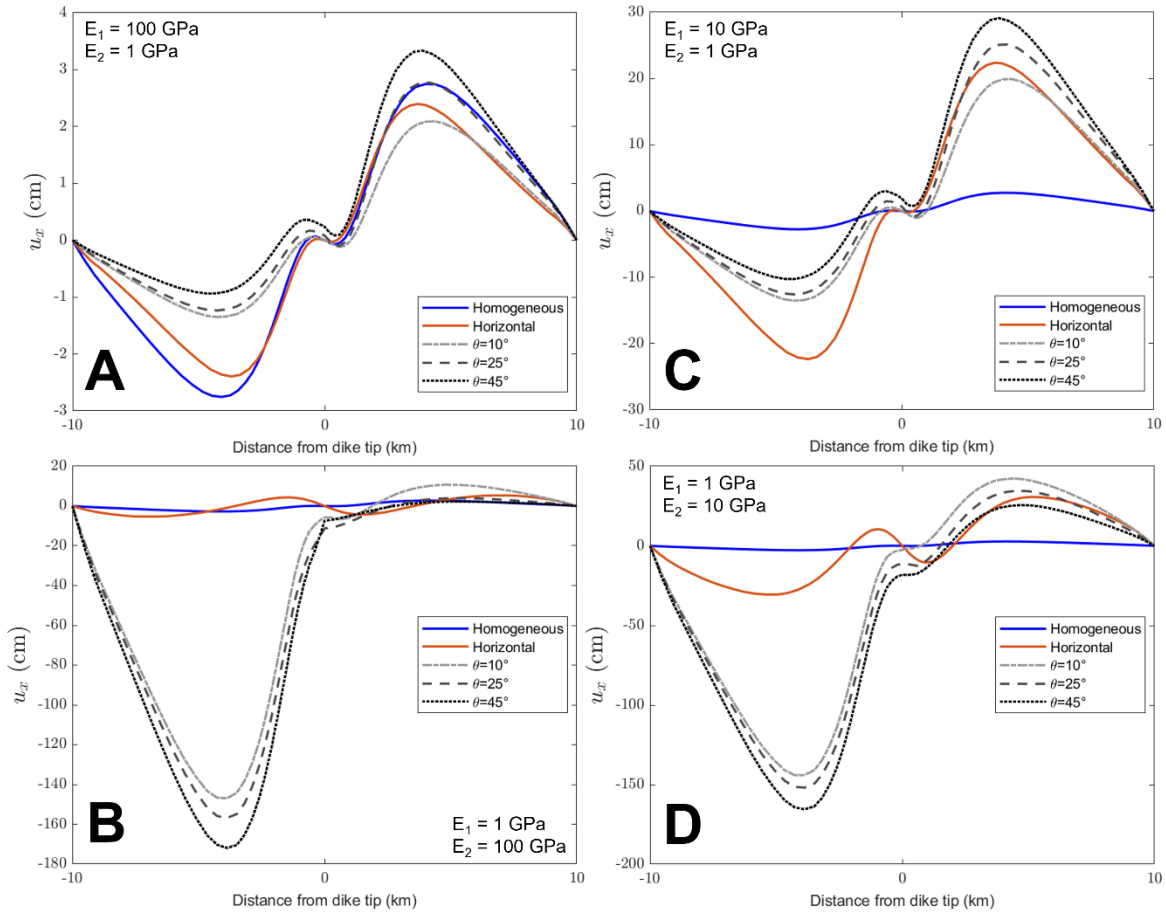

Figure 3: Horizontal ground displacement (u_x) variations relative to the lateral distance from the dike tip for each layer inclination and stiffness contrasts tested.

DISCUSSION AND CONCLUSION

The results indicate that for any study attempting to invert ground deformation measurements to determine dike emplacement processes, it is necessary to constrain, as best as possible, both the mechanical properties of the geological units and their attitudes, especially the amount by which the layers dip. Figure 4 shows the change in vertical and horizontal ground deformation with respect to the homogeneous cases recorded for each tested stiffness ratio and layer inclination. The comparison highlights that layer inclination, in the stiff to compliant setup (high E_1, low E_2), is a principal contributor to increasing surface deformation, while in the compliant to stiff setup (low E_1, high E_2) is a principal contributor

to decrease surface deformation. A series of model fits can describe the relationship between ground displacements, layer inclination and its mechanical properties. We suggest that when the geology of a volcanic zone is well-characterized in terms of the rock mechanical properties and attitudes, it should be possible to derive a similar series of curves so as to be able to estimate the contribution of the component of ground deformation associated specifically with the layered sequence amplification effect reported.

Our numerical results can be explained by considering the area, or in geological terms the volume, of the different modeled rock layers. The angle at which each individual unit dips will play a role in the volume of material available for deformation since the area of the upper layer changes depending on the angle of inclination (Figure 4C). The deformation amount increases or decreases because the area of the stiff layer reduces or increases with respect to the area of the compliant layer. As we show in our results, the larger the area of the stiff unit, the less the deformation and vice versa, and in these simplistic models it is the angle of inclination of the contact between the units which controls the area. It is then expected, and quantifiable, that the area over which compliant or stiff rocks are located will deform more or less as a function of both the rocks Young's modulus and area. In nature, the calculation of layer areas would likely be more complex and involve multiple layers, but the physical processes described here remain. Further work should aim to fully characterize both the mechanical properties and layer geometries of crustal zones hosting volcanoes in order to delineate their relative influence on recorded surface deformation.

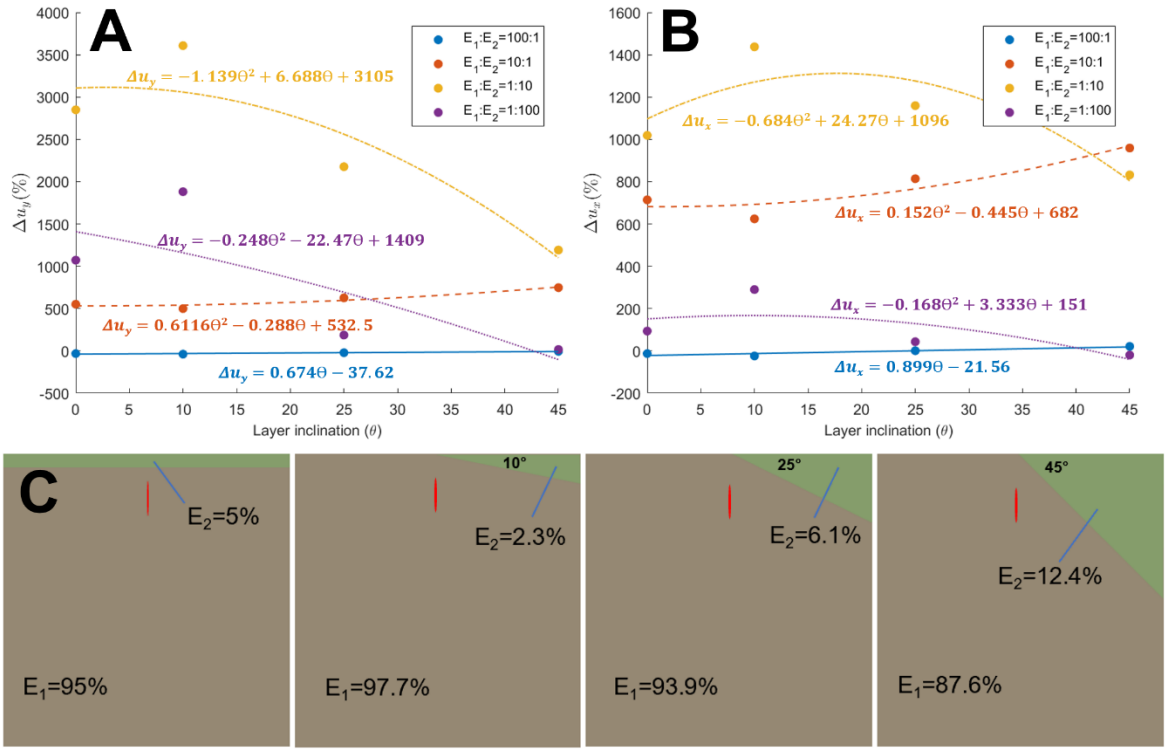

Figure 4: A) and B): Change in the vertical (Δu_y) and horizontal displacement (Δu_y) in percentages with respect to the homogeneous (elastic half-space) model for each layer inclination and stiffness ratio tested (E_1:E_2). C) Diagrams showing the area ratio in percentages between the two modeled crustal segments for the different angles of inclination.

Our models have shown that the combination of mechanical heterogeneity (e.g., Masterlark, 2007) and layer inclination can substantially alter dike-induced ground deformation signals which can become highly asymmetric and as much as 30 times different than if assuming a homogeneous elastic half-space model. The asymmetric ground deformation profiles demonstrated are similar to those generated in other numerical and analogue models of inclined sheet emplacement (i.e Kavanagh et al., 2018; Bazargan and Gudmundsso, 2020). This suggests that it is equally important to consider the geometry of the rock units into which a magmatic intrusion emplaces as well as the intrusion geometry because similar deformation

signals could be generated by vertical or inclined intrusions depending on the presence of inclined and stratified layered sequence. Whilst in our models the ground surface is flat, further complexities may arrive when introducing both topography (e.g., Trasatti et al., 2003; Johnson et al., 2019) with layer inclination and so this should be further investigated. Other studies (e.g., Magee et al., 2017, Poppe et al., 2019) have shown that deformation can be partly accommodated by fractures surrounding magmatic intrusions which also influence surface deformation signals. We do not consider such dislocations or inelastic deformations but combined with the data presented here further highlight the need to accurately characterize crustal structure to correctly determine intrusive processes. Furthermore, Masterlark (2007) suggests that differences in Poisson's ratio between layers can alter deformation signals by as much as 40% and so combining such properties into inclined layer models may also be of value. Ultimately, to test such models more must be known about the stratigraphy underlying volcanoes and the variation in mechanical properties of the geological units (e.g., Kendrick et al., 2021). Our models could be tested using analogue techniques (e.g., Kavanagh et al., 2018) and a dedicated volcano deformation study combining these data with ground deformation measurements is paramount.

ACKNOWLEDGEMENTS

This research was funded by ANID, through FONDECYT project 11190143 and by the Clover 2030 Open-Seed Fund. MC acknowledges support from ANID Scholarship 21202065. JK acknowledges a UKRI Future Leaders Fellowship (MR/S035141/1).

REFERENCES CITED

Acocella, V, 2021, Volcano-tectonic Processes. Advances in Volcanology, Springer-Nature, Heidelberg, 537 p.

Bazargan, M., and Gudmundsson, A., 2019. Dike-induced stresses and displacements in layered volcanic zones. Journal of Volcanology and Geothermal Research, 384, 189-205.

Bazargan, M., and Gudmundsson, A., 2020, Stresses and displacements in layered rocks induced by inclined (cone) sheets. Journal of Volcanology and Geothermal Research, 401, 106965.

Clunes, M., Browning, J., Cembrano, J., Marquardt, C., and Gudmundsson, A., 2021, Crustal folds alter local stress fields as demonstrated by magma sheet—Fold interactions in the Central Andes. Earth and Planetary Science Letters, 570, 117080.

Drymoni, K., Browning, J., and Gudmundsson, A., 2020, Dyke-arrest scenarios in extensional regimes: Insights from field observations and numerical models, Santorini, Greece. Journal of Volcanology and Geothermal Research, 396, p.106854.

Geshi, N., Browning, J., and Kusumoto, S, 2020, Magmatic overpressures, volatile exsolution and potential explosivity of fissure eruptions inferred via dike aspect ratios. Scientific reports, 10(1), 1-9.

Gudmundsson, A, 1983, Form and dimensions of dykes in eastern Iceland. *Tectonophysics*, *95*(3-4), 295-307.

Gudmundsson, A., Marinoni, L.B., and Marti, J., 1999, Injection and arrest of dykes: implications for volcanic hazards. Journal of Volcanology and Geothermal Research, 88(1-2), pp.1-13.

Gudmundsson, A., 2002, Emplacement and arrest of sheets and dykes in central volcanoes. Journal of Volcanology and Geothermal Research, 116(3-4), 279-298.

Gudmundsson, A., and Philipp, S. L., 2006, How local stress fields prevent volcanic eruptions. Journal of Volcanology and Geothermal research, 158(3-4), 257-268.

Gudmundsson, A., 2011, Rock fractures in geological processes. Cambridge University Press. 578.

Gudmundsson, A., 2020, Volcanotectonics: Understanding the Structure, Deformation and Dynamics of Volcanoes. Cambridge: Cambridge University Press. doi:10.1017/9781139176217

Johnson, J. H., Poland, M. P., Anderson, K. R., and Biggs, J., 2019. A cautionary tale of topography and tilt from Kilauea Caldera. Geophysical Research Letters, 46(8), 4221-4229.

Kavanagh, J.L., Burns, A.J., Hazim, S.H., Wood, E.P., Martin, S.A., Hignett, S. and Dennis, D.J., 2018, Challenging dyke ascent models using novel laboratory experiments: Implications for reinterpreting evidence of magma ascent and volcanism. Journal of Volcanology and Geothermal Research, 354, pp.87-101.

Kendrick, J.E., Schaefer, L.N., Schauroth, J., Bell, A.F., Lamb, O.D., Lamur, A., Miwa, T., Coats, R., Lavallée, Y. and Kennedy, B.M., 2021, Physical and mechanical rock properties of a heterogeneous volcano: the case of Mount Unzen, Japan. Solid Earth, 12(3), pp.633-664.

Maccaferri, F., Bonafede, M. and Rivalta, E., 2010, A numerical model of dyke propagation in layered elastic media. Geophysical Journal International, 180(3), pp.1107-1123.

Magee, C., Bastow, I.D., van Wyk de Vries, B., Jackson, C.A.L., Hetherington, R., Hagos, M., and Hoggett, M., 2017, Structure and dynamics of surface uplift induced by incremental sill emplacement. Geology, 45(5), 431-434.

Masterlark, T., 2007, Magma intrusion and deformation predictions: Sensitivities to the Mogi assumptions. *Journal of Geophysical Research: Solid Earth*, *112*(B6).

Mogi, K., 1958, Relations between the eruptions of various volcanoes and the deformations of the ground surface around them, Bull. Earthquake Res. Inst. Univ. Tokyo, 36, 99–134.

Okada, Y., 1985, Surface deformation due to shear and tensile faults in a half-space. *Bulletin of the seismological society of America*, *75*(4), 1135-1154.

Poppe, S., Holohan, E. P., Galland, O., Buls, N., Van Gompel, G., Keelson, B., Tournigand, P., Brancart, J., Hollis, D., Nila, A., and Kervyn, M., 2019, An inside perspective on magma intrusion: Quantifying 3D displacement and strain in laboratory experiments by dynamic X-ray computed tomography. *Frontiers in Earth Science*, *7*, 62.

Rivalta, E., Taisne, B., Bunger, A.P. and Katz, R.F., 2015, A review of mechanical models of dike propagation: Schools of thought, results and future directions. Tectonophysics, 638, pp.1-42.

Sparks, R. S. J., Biggs, J., and Neuberg, J. W, 2012, Monitoring volcanoes. *Science*, *335*(6074), 1310-1311.

Trasatti, E., Giunchi, C., and Bonafede, M., 2003, Effects of topography and rheological layering on ground deformation in volcanic regions. Journal of Volcanology and Geothermal Research, 122(1-2), 89-110.

Supplemental Material

Inclination and heterogeneity of layered geological sequences influence dike-induced ground deformation

Matías Clunes[1], John Browning[1, 2, 3], Carlos Marquardt[1, 3], Jorge Cortez[1], Kyriaki Drymoni[4], and Janine Kavanagh[5]

[1]Department of Structural and Geotechnical Engineering, Pontificia Universidad Católica de Chile, Santiago, Chile

[2]Andean Geothermal Centre of Excellence (CEGA), Universidad de Chile, Santiago, Chile

[3]Department of Mining Engineering, Pontificia Universidad Católica de Chile, Santiago, Chile

[4]Department of Earth and Environmental Sciences, Università degli Studi di Milano-Bicocca, Milan, Italy

[5]School of Environmental Sciences, University of Liverpool, Liverpool, United Kingdom

EXTENDED NUMERICAL MODEL SETUP

Domain size effect

We concentrate only on the results using the domain size specified in the numerical model setup (20 km wide x 20 km deep) but comparisons with larger domain sizes are given Figures S1 and S2. Whilst the total amounts of absolute surface deformation do alter between models with different sized domains, the changes in deformation with heterogeneity and layer inclination, the focus of this work, remain broadly similar regardless of the domain size.

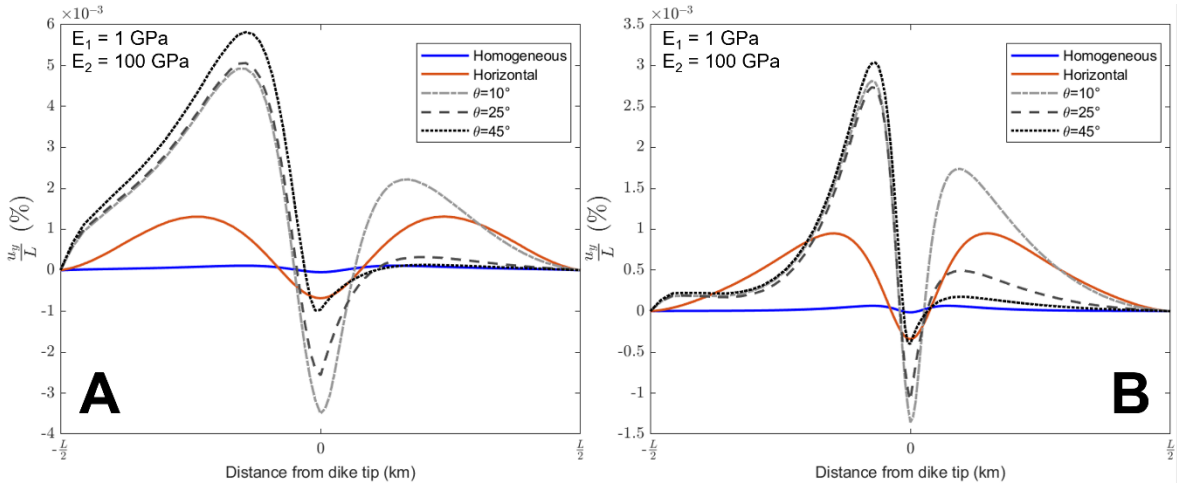

Figure S1: Comparison of vertical ground displacement (u_y) variations in percentage relative to the lateral distance from the dike tip obtained from A) domain size of 20 km wide and 20 km deep and B) domain size of 40 km wide and 40 km deep. The displacements are normalised to the domain length (L).

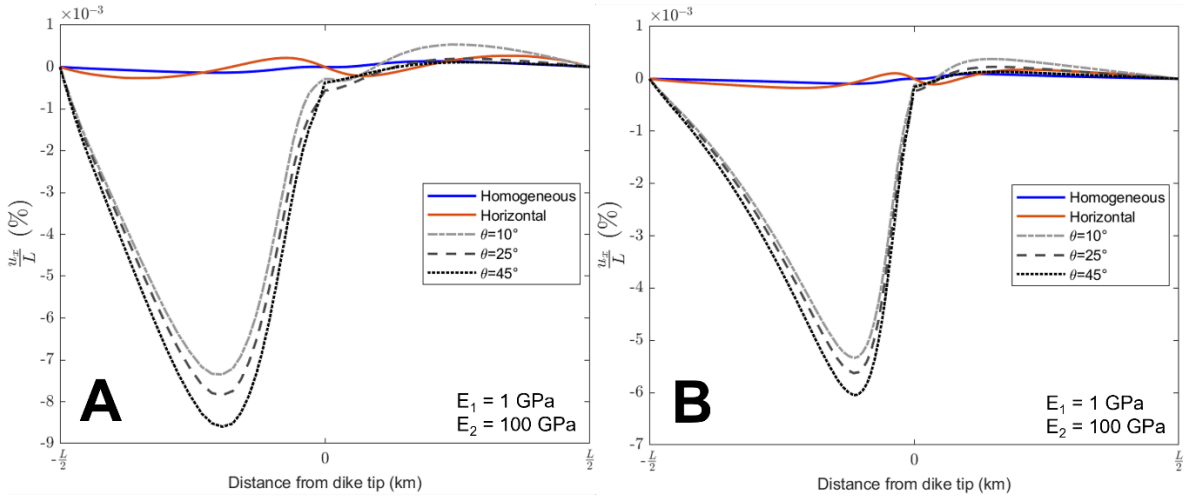

Figure S2: Comparison of horizontal ground displacement variations (u_x) in percentage relative to the lateral distance from the dike tip obtained from A) domain size of 20 km wide and 20 km deep and B) domain size of 40 km wide and 40 km deep. The displacements are normalised to the domain length (L).

Overpressure

In all models we used an overpressure of 5 MPa chosen since this represents a value within the range of host rock tensile strengths which are commonly between around 0.5 to 9 MPa (Amadei and Stephansson, 1997; Gudmundsson, 2011; Gudmundsson, 2020) and so could be reasonably associated with dike emplacement. Since our study is concerned with defining the influence of layer inclination on surface deformation, we do not present results related to changes in magmatic overpressure, doing so would change the absolute surface deformation values but the patterns on deformation and layer influence remains the same.

Young's modulus ratios

In nature differences in stiffness are reflective of mechanically stratified volcanic sequences that host stiff units such as lava flows and intrusive rocks, and compliant units such as ash or poorly welded tuff. Whilst in reality some of the Young's modulus contrasts used in our work may be extreme (Heap et al., 2020), since we are interested in the general deformation behavior, we used combinations between 3 orders of magnitude of Young's modulus values (1, 10 and 100 GPa) to probe the full range of possibilities with the acknowledgement that to be applied to any geological unit of interest the rocks should be analytically tested and represents the order of magnitudes which can be found at layered volcanic edifices, such as stratovolcanoes (Gudmundsson, 2020).

Other parameters

We did not assign mechanical properties to the contacts between the layers and density (2700 kg/m^3) and Poisson's ratio (0.25) (Gudmundsson, 2011) of all layers were the same across all the model runs. We modeled the homogeneous crustal segment with a stiffness of 50 GPa chosen because it is close to the average value used between the stiffer (100 GPa) and the more compliant Young's modulus tested (1 GPa).

Area of the modeled layers

The 2D area of the dipping layers varies in the models as a function of inclination angle. The horizontal layer has an area of 20 km^2 which represents the 5% of the crustal segment modeled, the layer inclined 10° 9.25 km^2 (2.3%), the layer inclined 25° 24.2 km^2 (6.1%) and the layer inclined 45° 49.5 km^2 (12.4%).

Case study locations

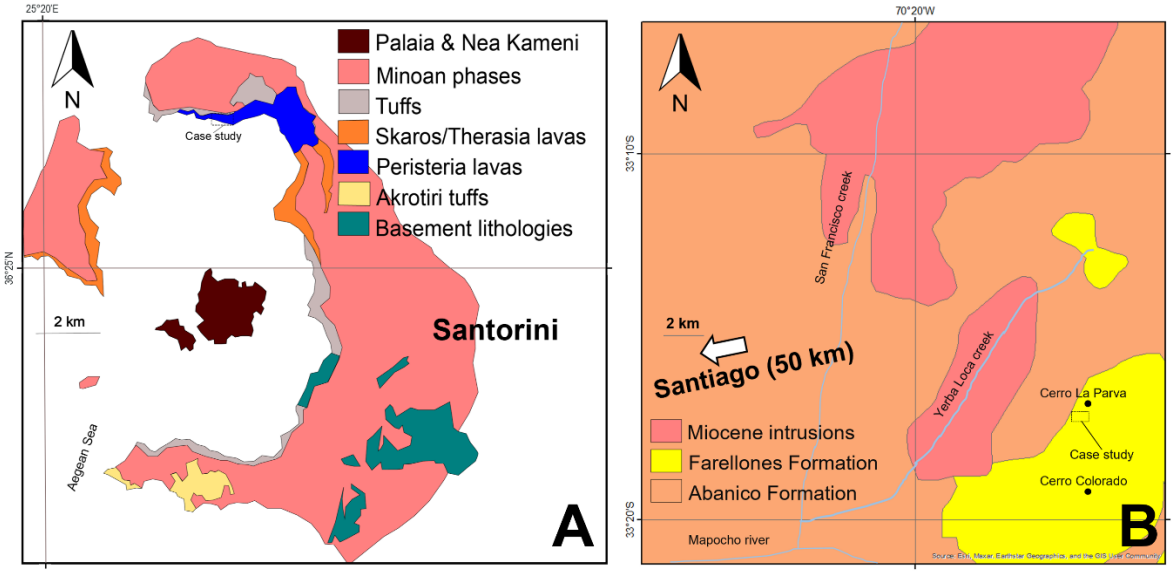

Figure S3: A) Simplified geological map from Santorini, Greece, modified from Druitt et al. (1999), where the case study from Figure 1D is located, at the northern caldera wall. B) Simplified geological map from the Andes of Central Chile, near to Santiago, modified from Rivano et al. (1990), where the case study from Figure 1E is located, at an outcrop of the Miocene volcanic rocks from Farellones Formation.

EXTENDED RESULTS

We focus only on this dike size and geometry to probe the relative influence of the surrounding host rock mechanical properties and layer inclination on the magnitude and extent of surface deformation. Our results show that whilst the magnitude of ground displacement varies with dike length and depth, the general patterns relating to layer heterogeneity and inclination are consistently observed for each dike length and depth modeled, but the extent of the absolute ground displacements is different, as expected (Figures S4-S19).

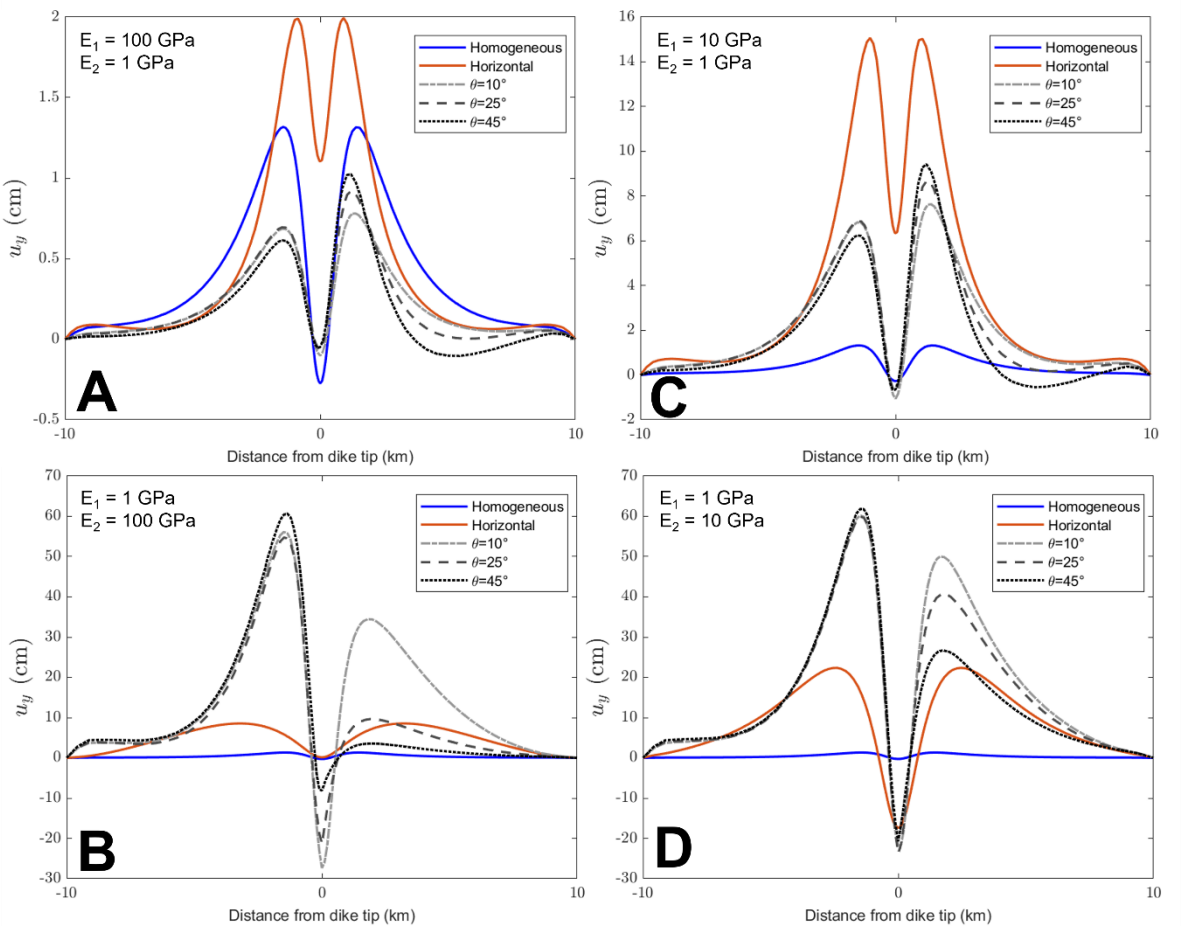

Figure S4: Vertical ground displacement (u_y) variations relative to the lateral distance from the dike tip for each of the modeled layer arrangements and stiffness contrasts tested. The modeled dike is 1 km in length and its upper tip is located at a depth of 1 km. The line colors indicate the geometry of the layers from homogeneous (i.e., where the segment is one material) to horizontal and inclined at 10, 25 and 45 degrees. In A) the stiffness contrast between the layer hosting the dike (E_1) and the inclined layer (E_2) is 100:1, in B) 1:100, in C) 10:1 and in D) 1:10.

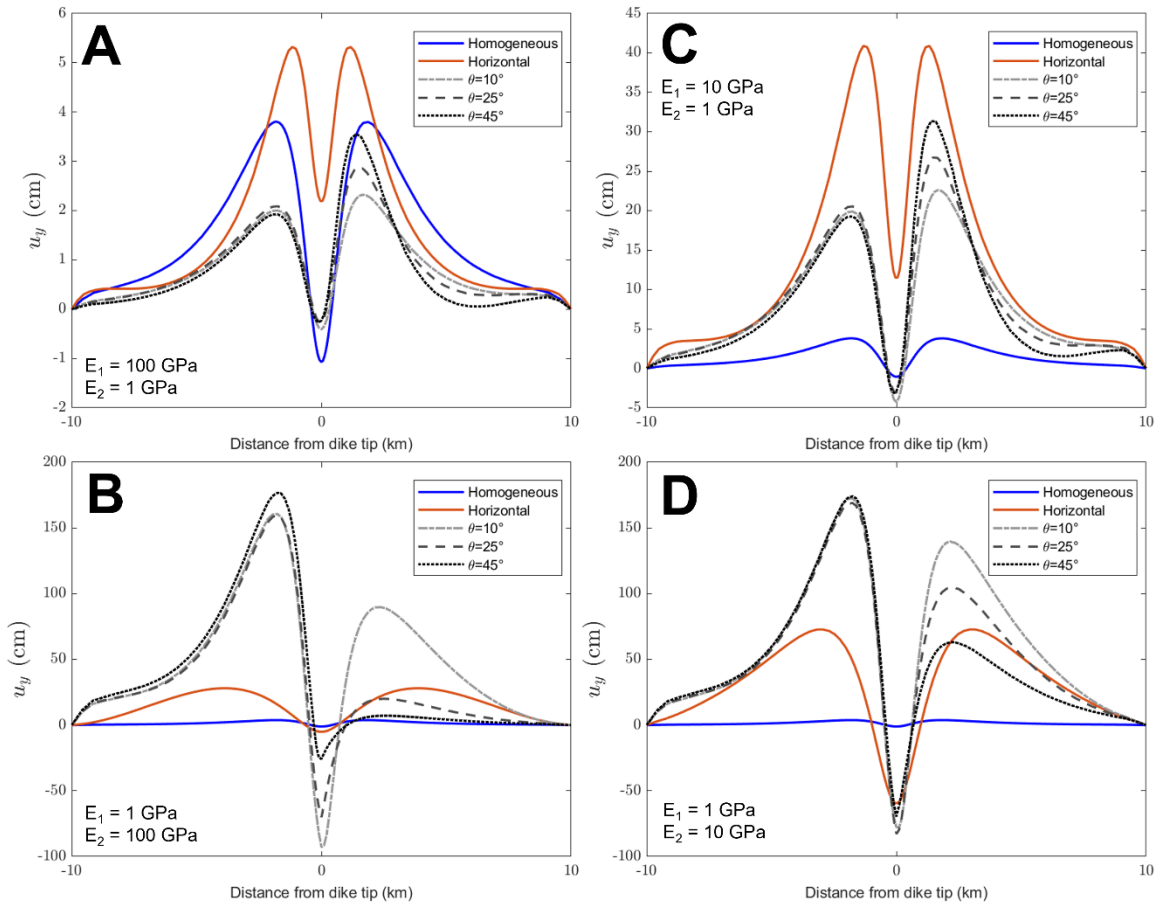

Figure S5: Vertical ground displacement (u_y) variations relative to the lateral distance from the dike tip for each of the modeled layer arrangements and stiffness contrasts tested. The

modeled dike is 2 km in length and its upper tip is located at a depth of 1 km. The line colors indicate the geometry of the layers from homogeneous (i.e., where the segment is one material) to horizontal and inclined at 10, 25 and 45 degrees. In A) the stiffness contrast between the layer hosting the dike (E_1) and the inclined layer (E_2) is 100:1, in B) 1:100, in C) 10:1 and in D) 1:10.

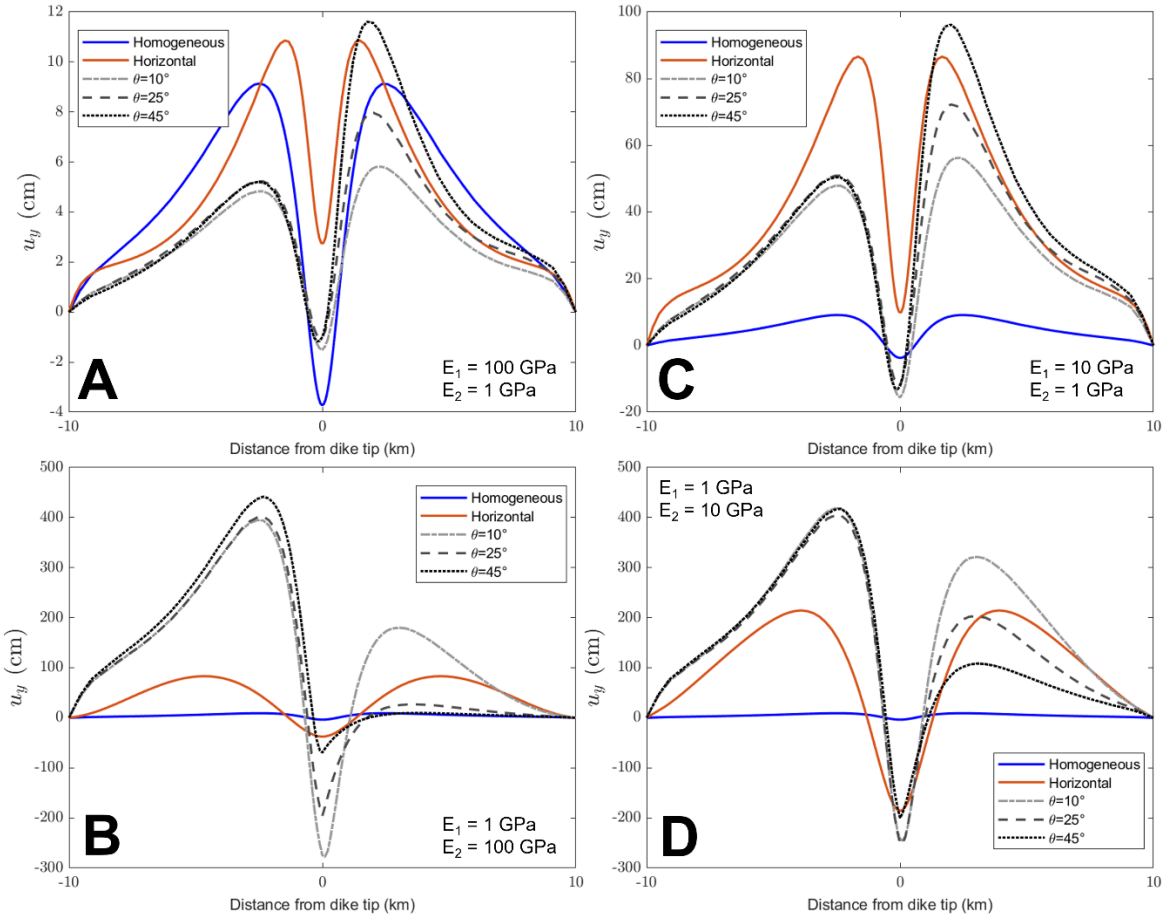

Figure S6: Vertical ground displacement (u_y) variations relative to the lateral distance from the dike tip for each of the modeled layer arrangements and stiffness contrasts tested. The modeled dike is 4 km in length and its upper tip is located at a depth of 1 km. The line colors indicate the geometry of the layers from homogeneous (i.e., where the segment is one

material) to horizontal and inclined at 10, 25 and 45 degrees. In A) the stiffness contrast between the layer hosting the dike (E_1) and the inclined layer (E_2) is 100:1, in B) 1:100, in C) 10:1 and in D) 1:10.

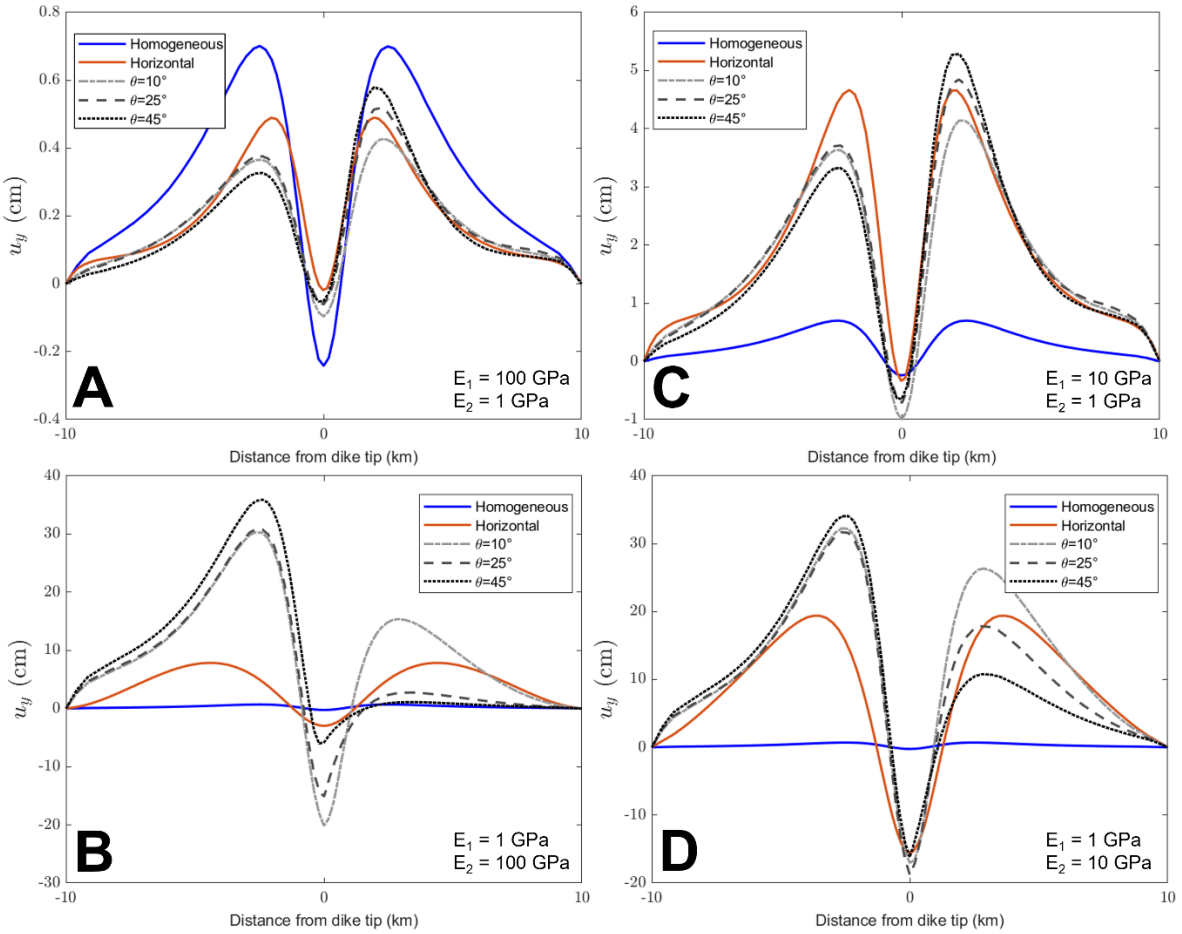

Figure S7: Vertical ground displacement (u_y) variations relative to the lateral distance from the dike tip for each of the modeled layer arrangements and stiffness contrasts tested. The modeled dike is 1 km in length and its upper tip is located at a depth of 2 km. The line colors indicate the geometry of the layers from homogeneous (i.e., where the segment is one material) to horizontal and inclined at 10, 25 and 45 degrees. In A) the stiffness contrast

between the layer hosting the dike (E_1) and the inclined layer (E_2) is 100:1, in B) 1:100, in C) 10:1 and in D) 1:10.

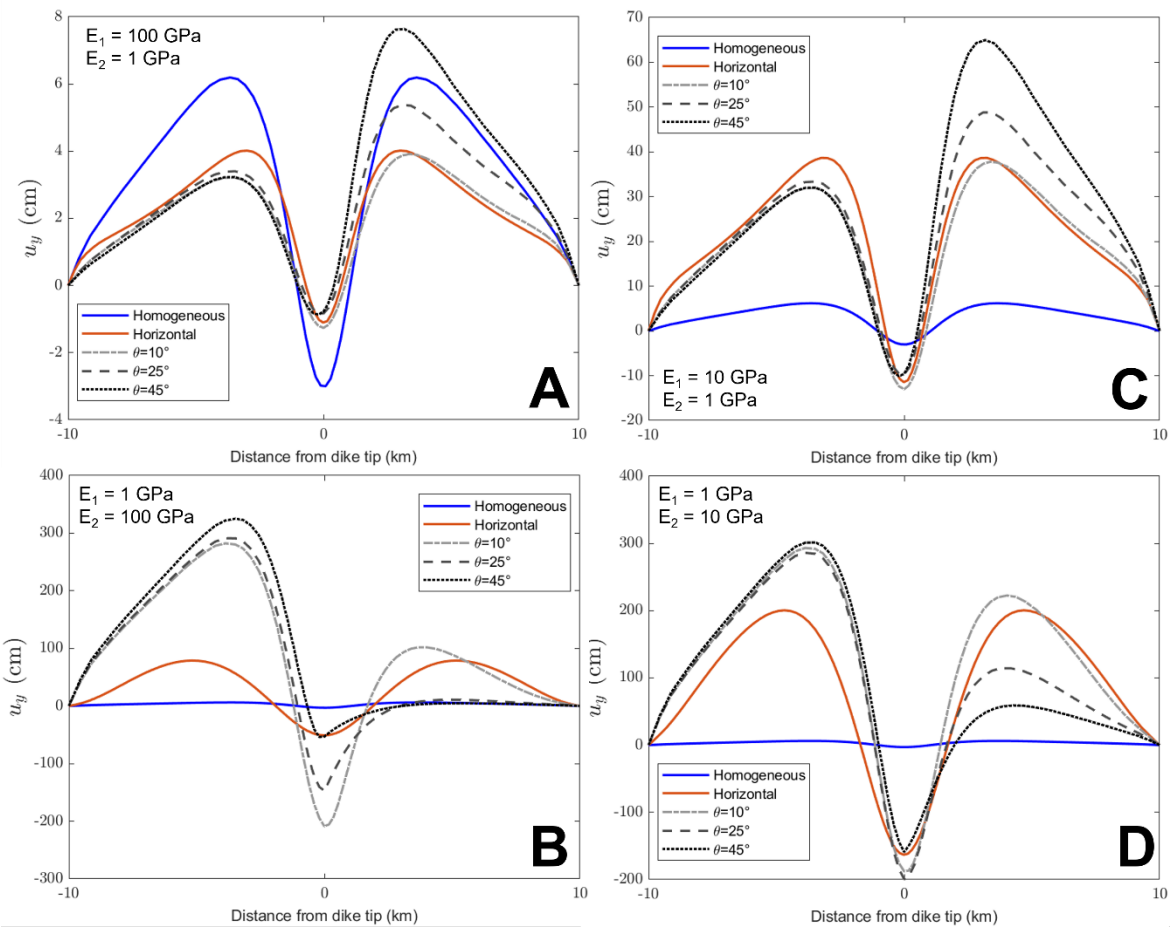

Figure S8: Vertical ground displacement (u_y) variations relative to the lateral distance from the dike tip for each of the modeled layer arrangements and stiffness contrasts tested. The modeled dike is 4 km in length and its upper tip is located at a depth of 2 km. The line colors indicate the geometry of the layers from homogeneous (i.e., where the segment is one material) to horizontal and inclined at 10, 25 and 45 degrees. In A) the stiffness contrast between the layer hosting the dike (E_1) and the inclined layer (E_2) is 100:1, in B) 1:100, in C) 10:1 and in D) 1:10.

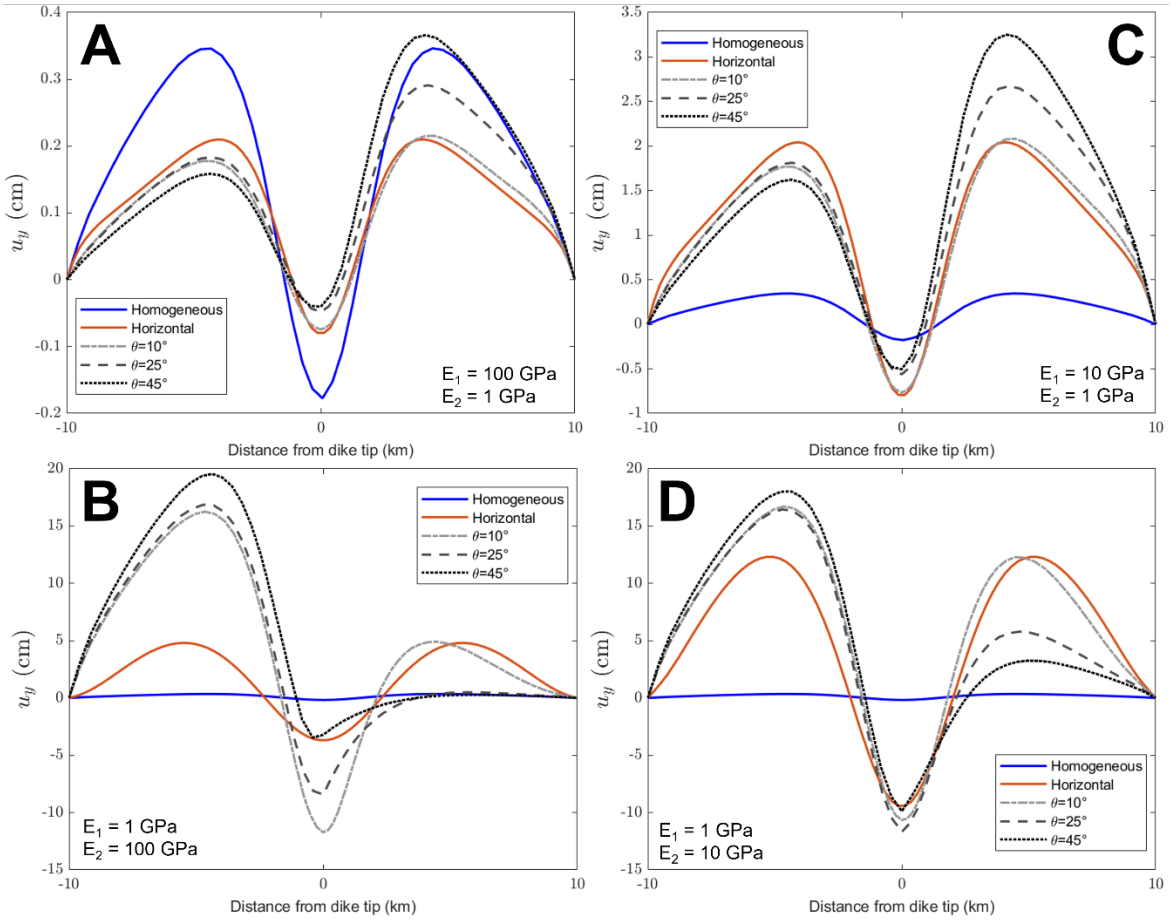

Figure S9: Vertical ground displacement (u_y) variations relative to the lateral distance from the dike tip for each of the modeled layer arrangements and stiffness contrasts tested. The modeled dike is 1 km in length and its upper tip is located at a depth of 4 km. The line colors indicate the geometry of the layers from homogeneous (i.e., where the segment is one material) to horizontal and inclined at 10, 25 and 45 degrees. In A) the stiffness contrast between the layer hosting the dike (E_1) and the inclined layer (E_2) is 100:1, in B) 1:100, in C) 10:1 and in D) 1:10.

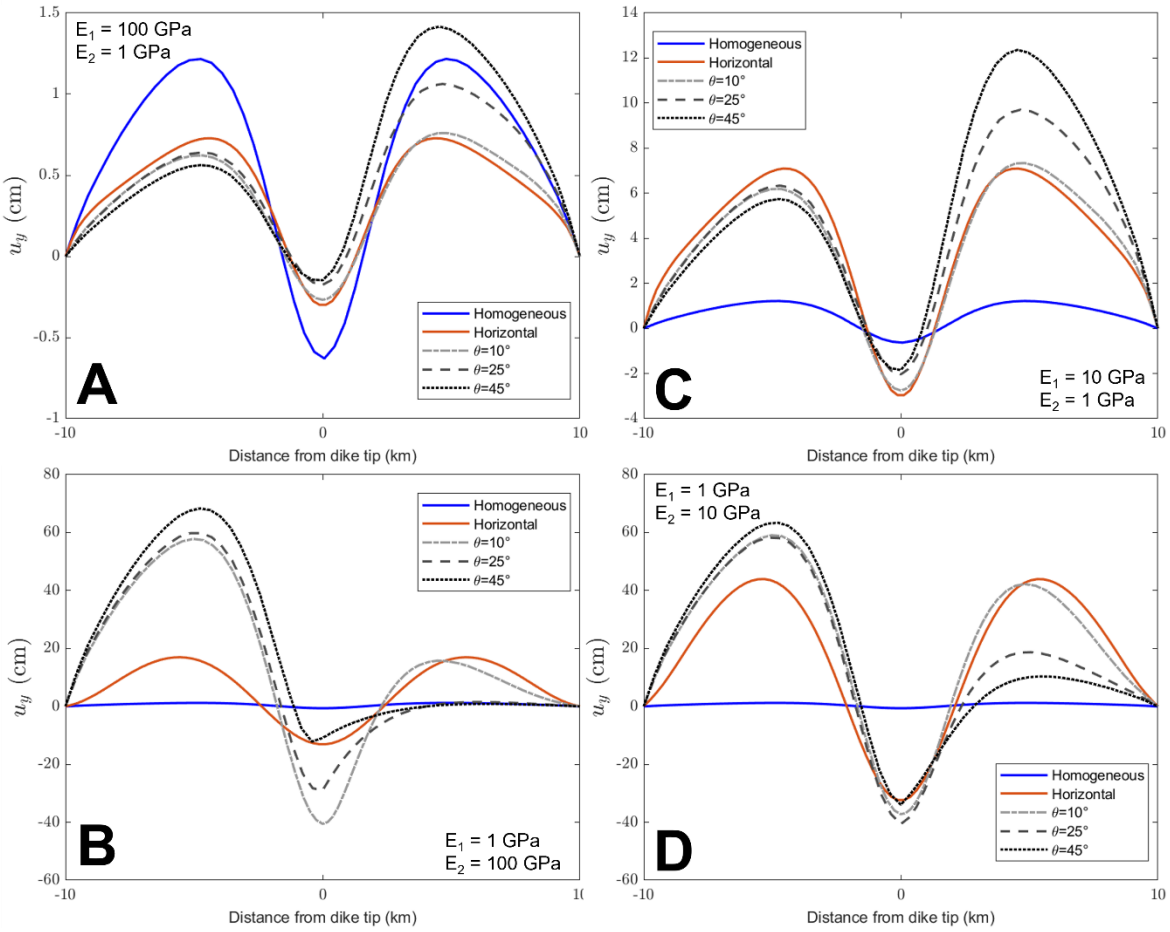

Figure S10: Vertical ground displacement (u_y) variations relative to the lateral distance from the dike tip for each of the modeled layer arrangements and stiffness contrasts tested. The modeled dike is 2 km in length and its upper tip is located at a depth of 4 km. The line colors indicate the geometry of the layers from homogeneous (i.e., where the segment is one material) to horizontal and inclined at 10, 25 and 45 degrees. In A) the stiffness contrast between the layer hosting the dike (E_1) and the inclined layer (E_2) is 100:1, in B) 1:100, in C) 10:1 and in D) 1:10.

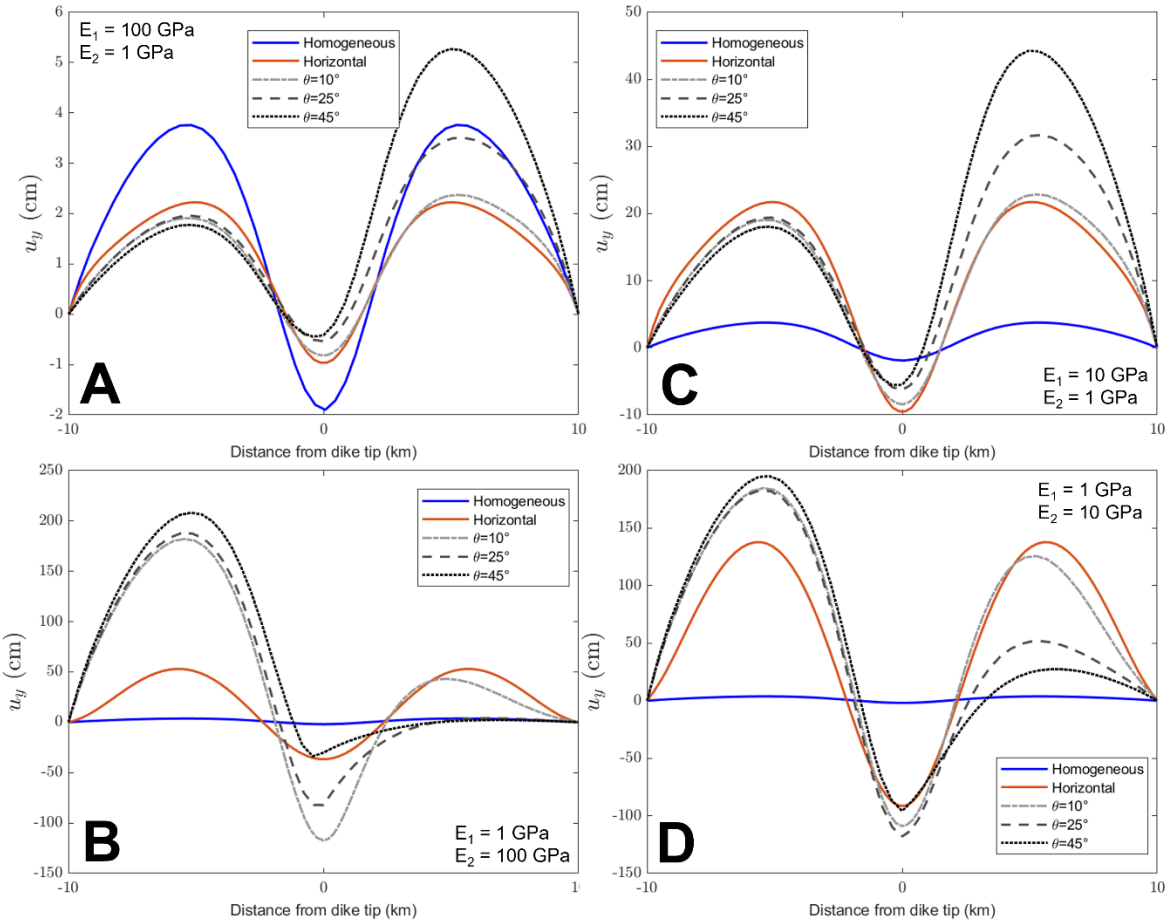

Figure S11: Vertical ground displacement (u_y) variations relative to the lateral distance from the dike tip for each of the modeled layer arrangements and stiffness contrasts tested. The modeled dike is 4 km in length and its upper tip is located at a depth of 4 km. The line colors indicate the geometry of the layers from homogeneous (i.e., where the segment is one material) to horizontal and inclined at 10, 25 and 45 degrees. In A) the stiffness contrast between the layer hosting the dike (E_1) and the inclined layer (E_2) is 100:1, in B) 1:100, in C) 10:1 and in D) 1:10.

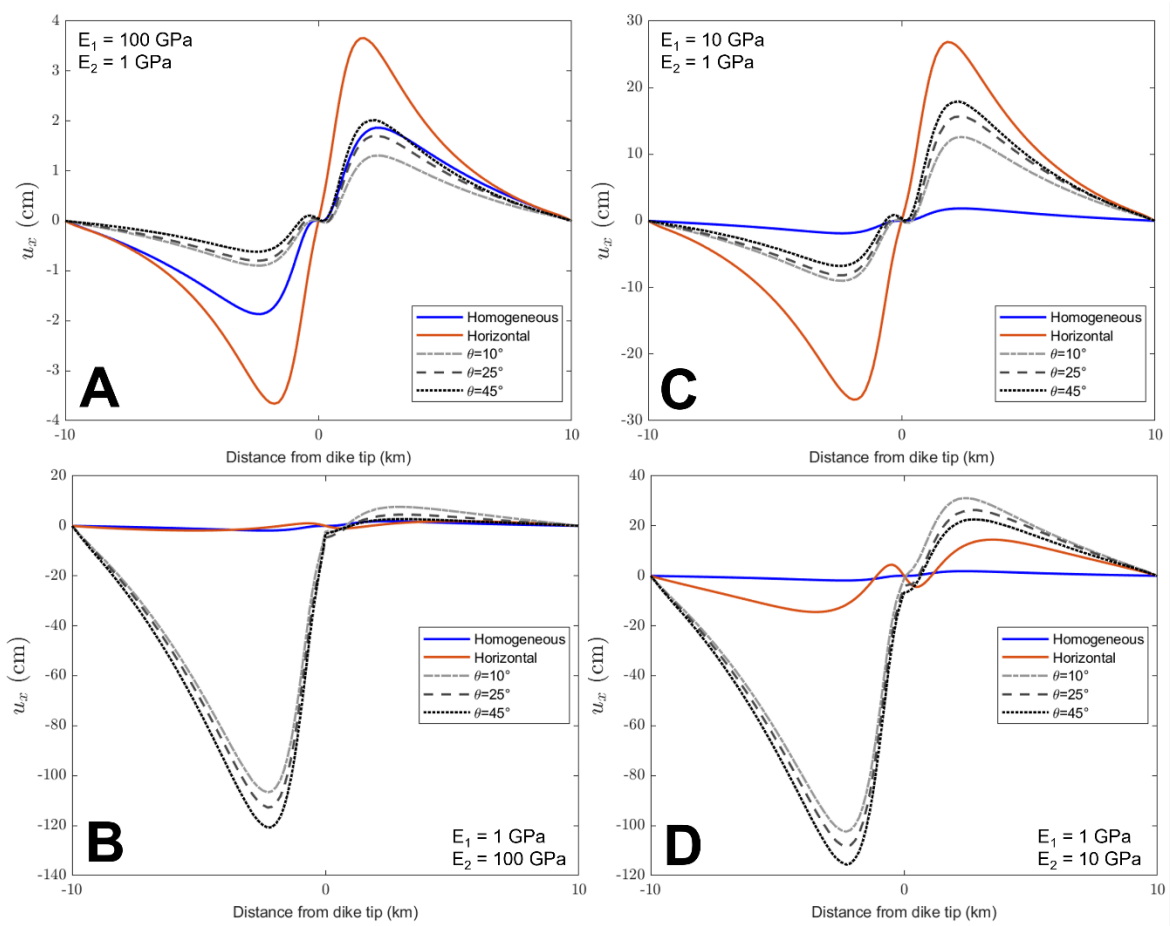

Figure S12: Horizontal ground displacement (u_x) variations relative to the lateral distance from the dike tip for each of the modeled layer arrangements and stiffness contrasts tested. The modeled dike is 1 km in length and its upper tip is located at a depth of 1 km. The line colors indicate the geometry of the layers from homogeneous (i.e., where the segment is one material) to horizontal and inclined at 10, 25 and 45 degrees. In A) the stiffness contrast between the layer hosting the dike (E_1) and the inclined layer (E_2) is 100:1, in B) 1:100, in C) 10:1 and in D) 1:10.

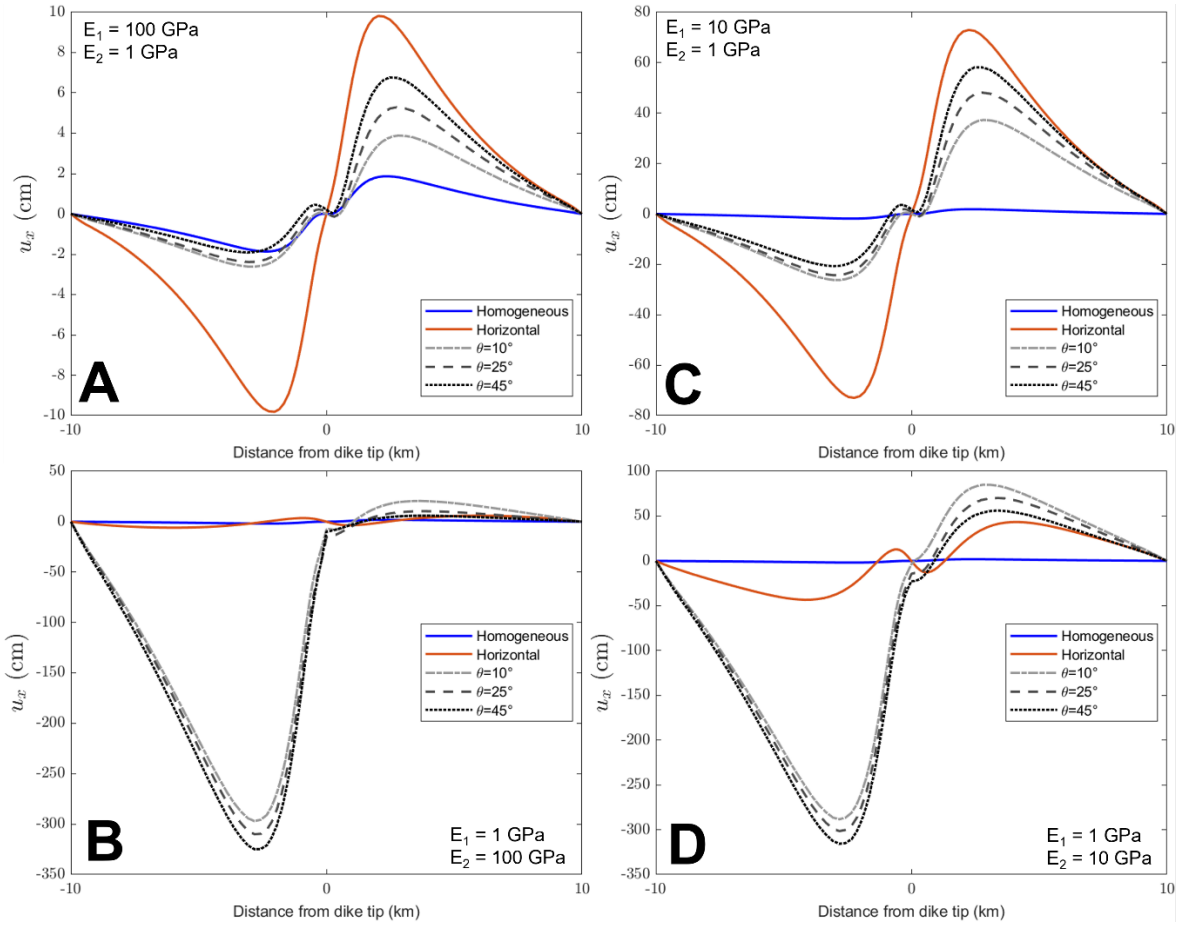

Figure S13: Horizontal ground displacement (u_x) variations relative to the lateral distance from the dike tip for each of the modeled layer arrangements and stiffness contrasts tested. The modeled dike is 2 km in length and its upper tip is located at a depth of 1 km. The line colors indicate the geometry of the layers from homogeneous (i.e., where the segment is one material) to horizontal and inclined at 10, 25 and 45 degrees. In A) the stiffness contrast between the layer hosting the dike (E_1) and the inclined layer (E_2) is 100:1, in B) 1:100, in C) 10:1 and in D) 1:10.

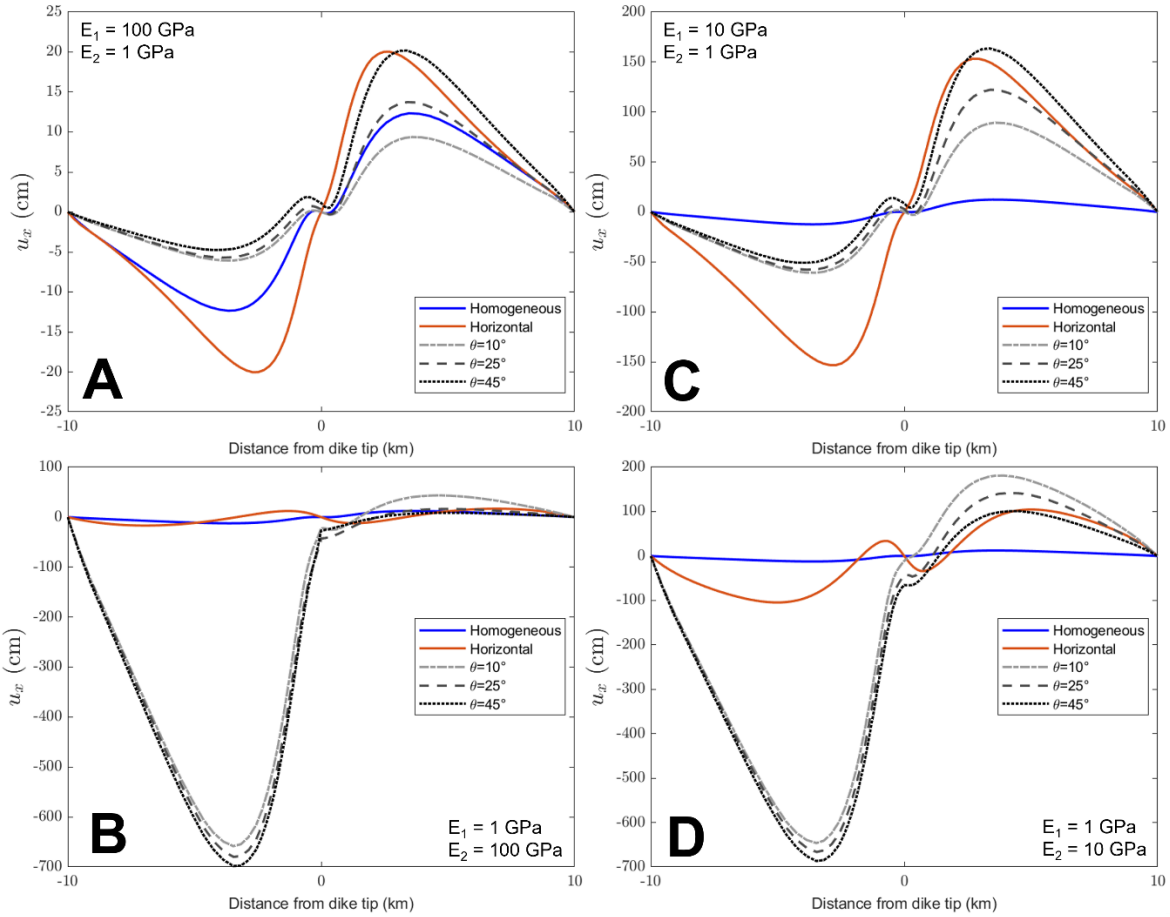

Figure S14: Horizontal ground displacement (u_x) variations relative to the lateral distance from the dike tip for each of the modeled layer arrangements and stiffness contrasts tested. The modeled dike is 4 km in length and its upper tip is located at a depth of 1 km. The line colors indicate the geometry of the layers from homogeneous (i.e., where the segment is one material) to horizontal and inclined at 10, 25 and 45 degrees. In A) the stiffness contrast between the layer hosting the dike (E_1) and the inclined layer (E_2) is 100:1, in B) 1:100, in C) 10:1 and in D) 1:10.

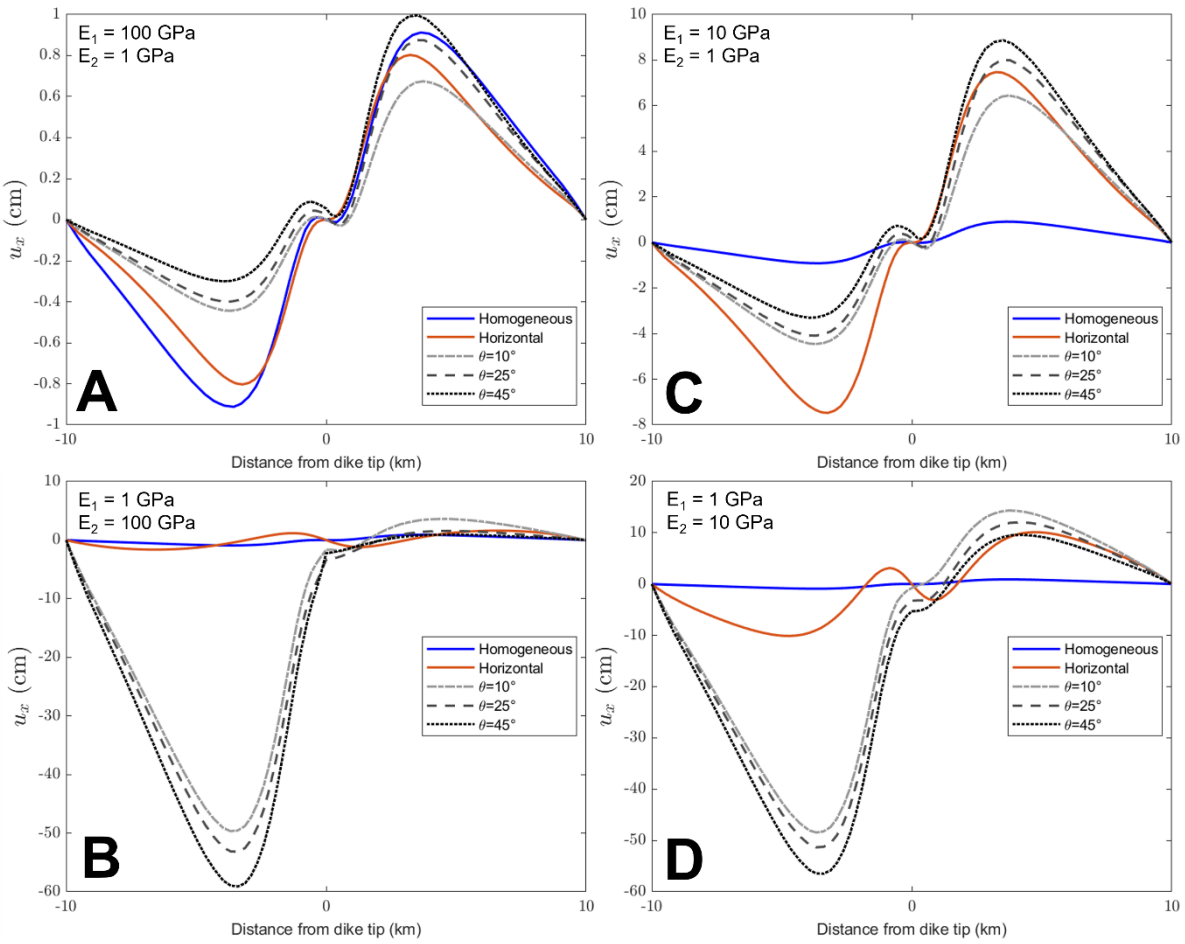

Figure S15: Horizontal ground displacement (u_x) variations relative to the lateral distance from the dike tip for each of the modeled layer arrangements and stiffness contrasts tested. The modeled dike is 1 km in length and its upper tip is located at a depth of 2 km. The line colors indicate the geometry of the layers from homogeneous (i.e., where the segment is one material) to horizontal and inclined at 10, 25 and 45 degrees. In A) the stiffness contrast between the layer hosting the dike (E_1) and the inclined layer (E_2) is 100:1, in B) 1:100, in C) 10:1 and in D) 1:10.

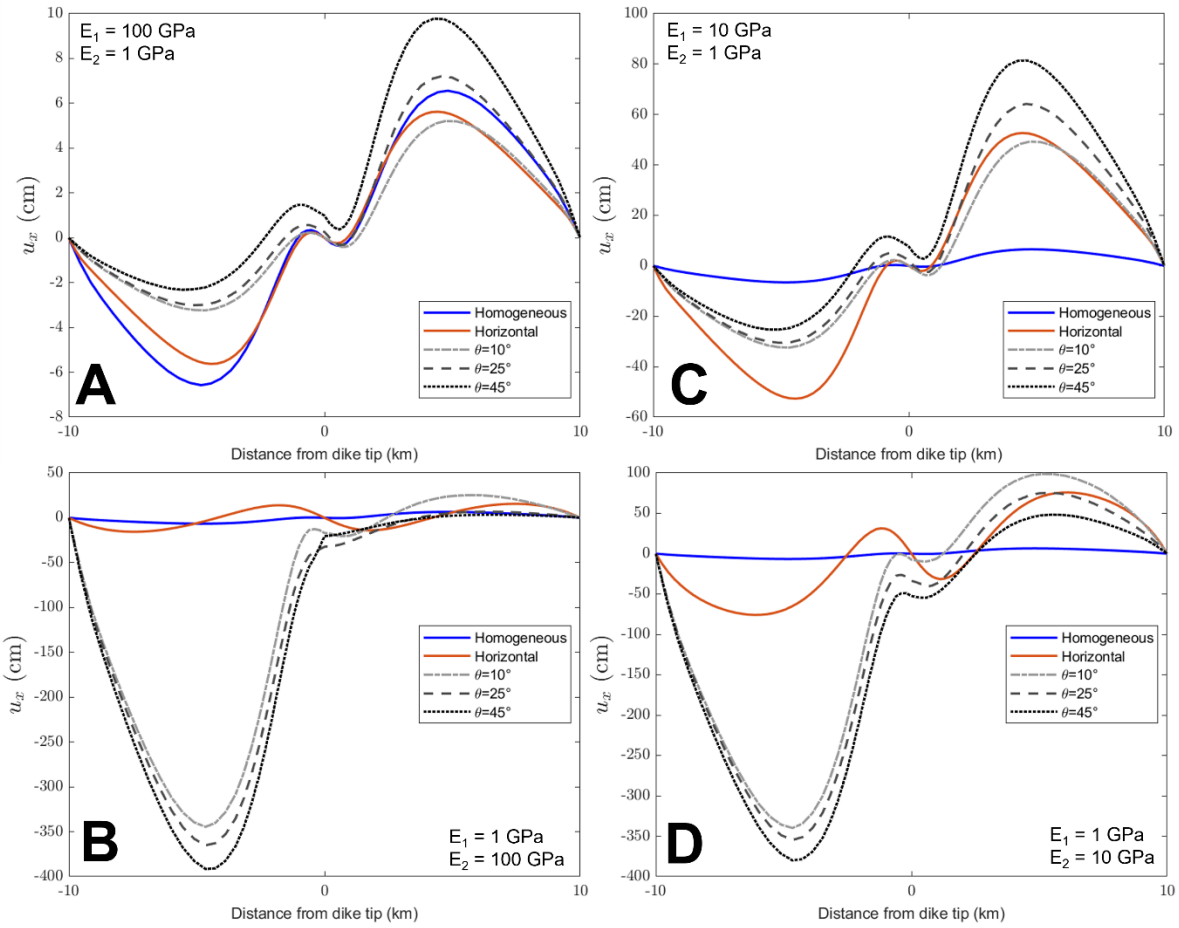

Figure S16: Horizontal ground displacement (u_x) variations relative to the lateral distance from the dike tip for each of the modeled layer arrangements and stiffness contrasts tested. The modeled dike is 4 km in length and its upper tip is located at a depth of 2 km. The line colors indicate the geometry of the layers from homogeneous (i.e., where the segment is one material) to horizontal and inclined at 10, 25 and 45 degrees. In A) the stiffness contrast between the layer hosting the dike (E_1) and the inclined layer (E_2) is 100:1, in B) 1:100, in C) 10:1 and in D) 1:10.

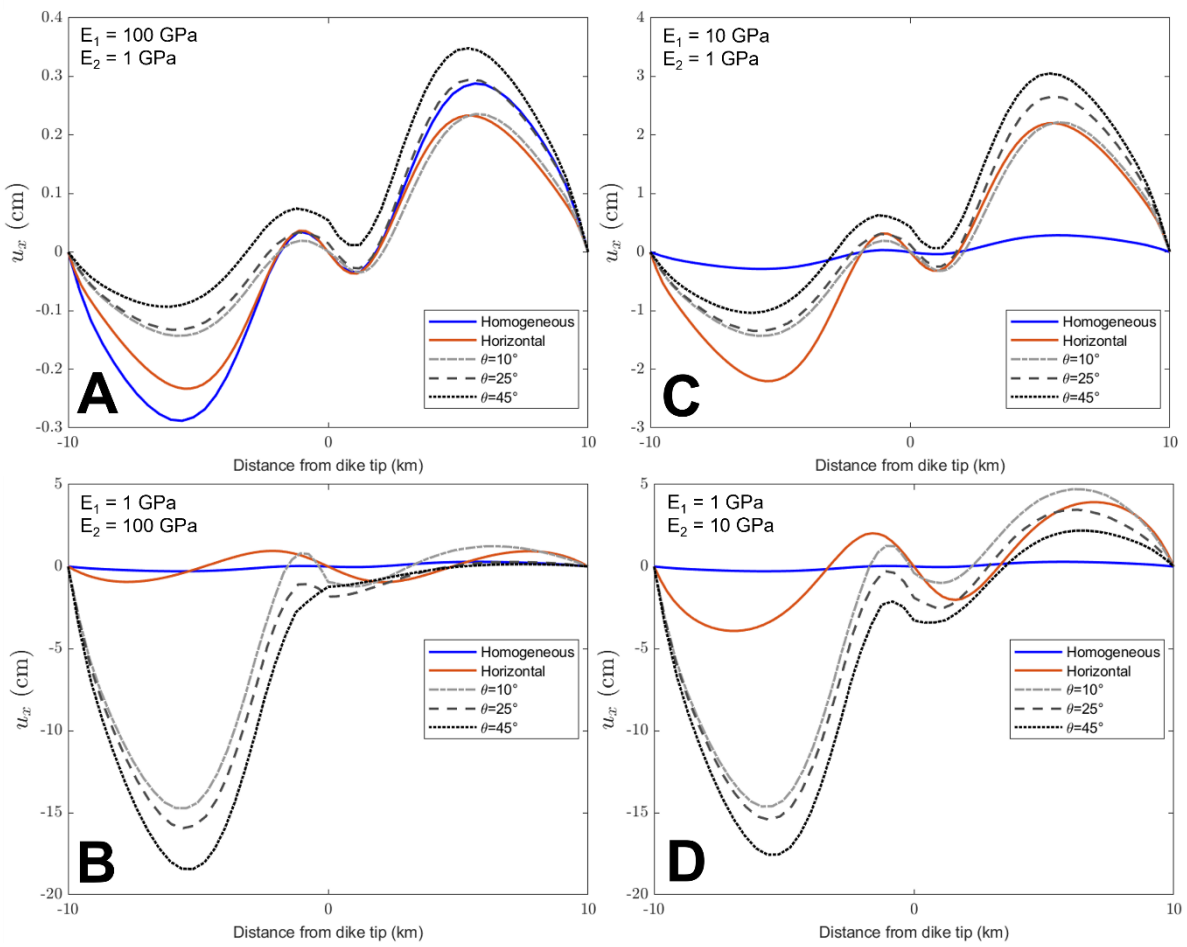

Figure S17: Horizontal ground displacement (u_x) variations relative to the lateral distance from the dike tip for each of the modeled layer arrangements and stiffness contrasts tested. The modeled dike is 1 km in length and its upper tip is located at a depth of 4 km. The line colors indicate the geometry of the layers from homogeneous (i.e., where the segment is one material) to horizontal and inclined at 10, 25 and 45 degrees. In A) the stiffness contrast between the layer hosting the dike (E_1) and the inclined layer (E_2) is 100:1, in B) 1:100, in C) 10:1 and in D) 1:10.

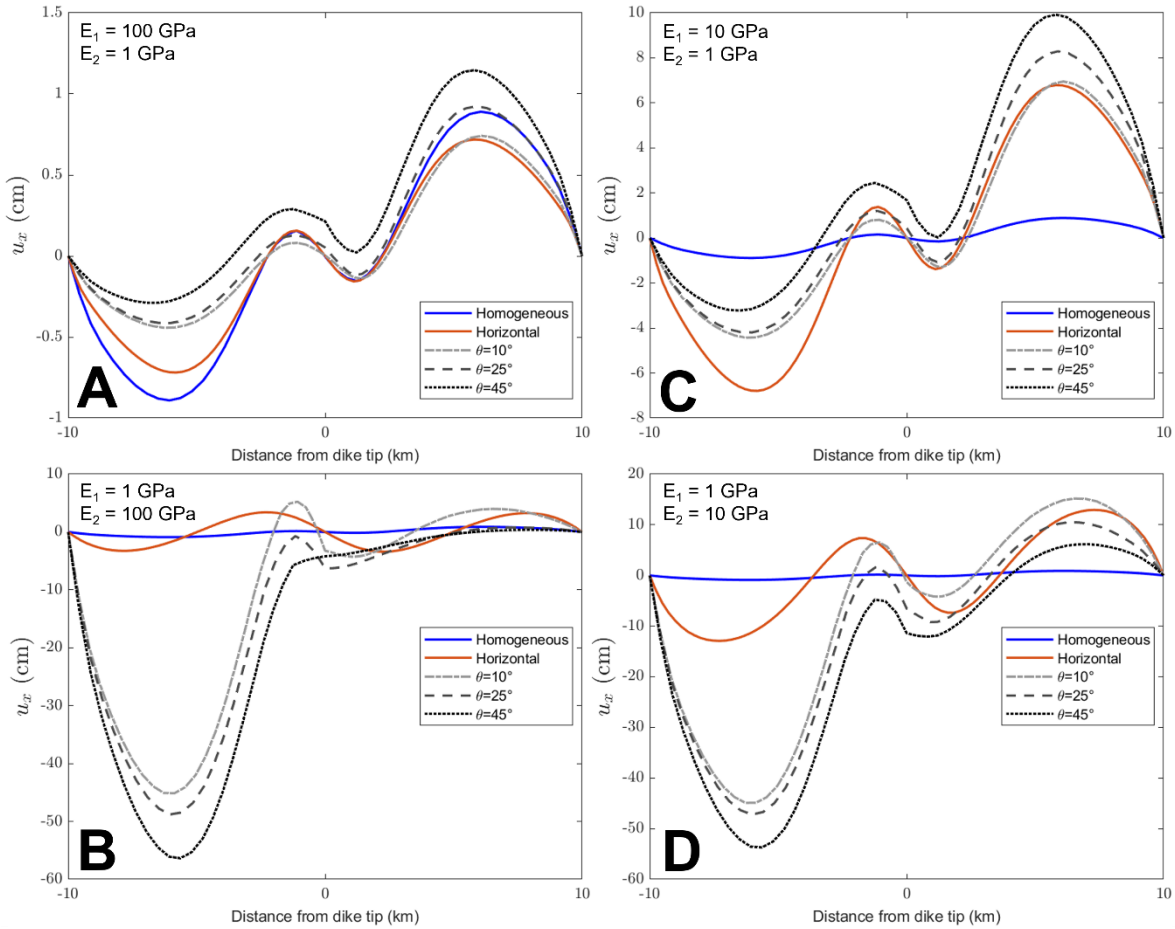

Figure S18: Horizontal ground displacement (u_x) variations relative to the lateral distance from the dike tip for each of the modeled layer arrangements and stiffness contrasts tested. The modeled dike is 2 km in length and its upper tip is located at a depth of 4 km. The line colors indicate the geometry of the layers from homogeneous (i.e., where the segment is one material) to horizontal and inclined at 10, 25 and 45 degrees. In A) the stiffness contrast between the layer hosting the dike (E_1) and the inclined layer (E_2) is 100:1, in B) 1:100, in C) 10:1 and in D) 1:10.

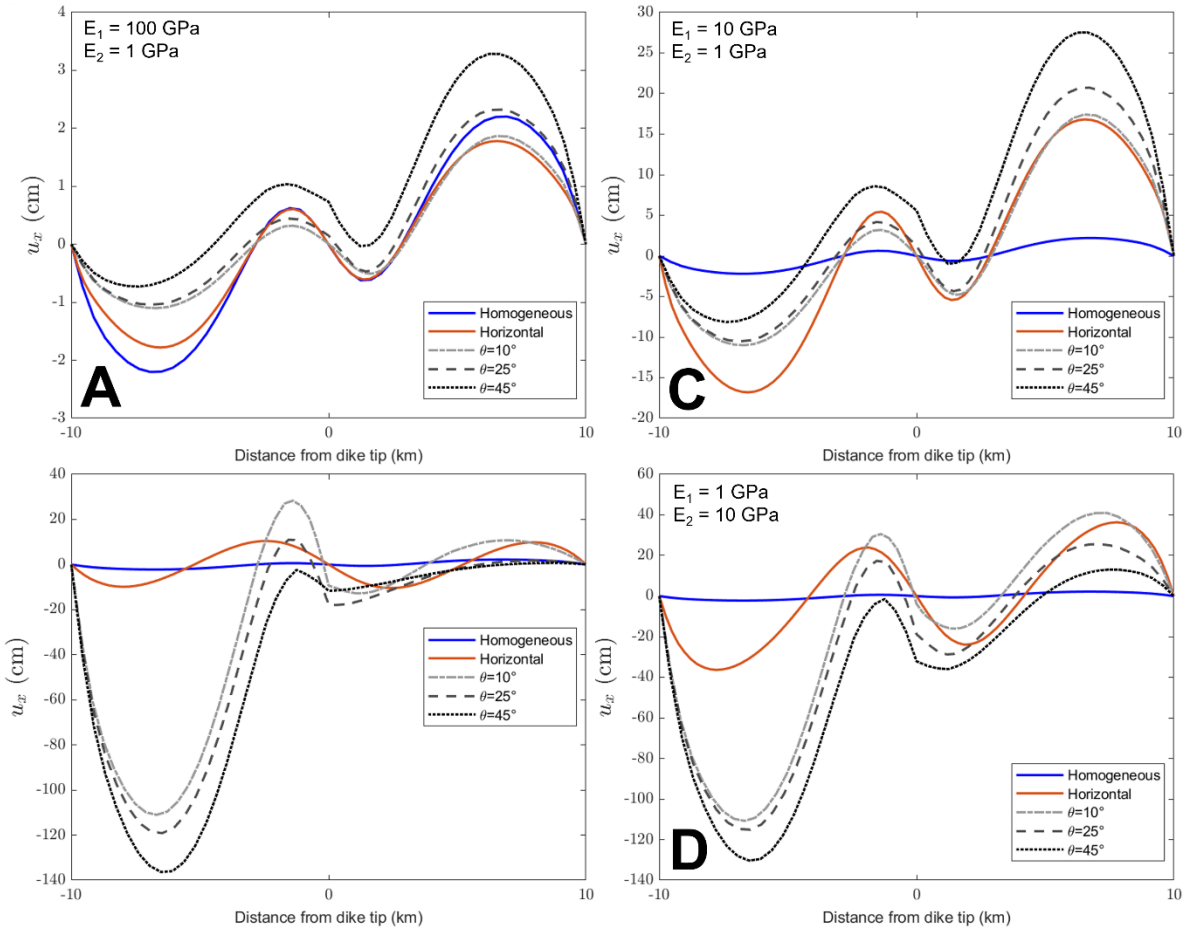

Figure S19: Horizontal ground displacement (u_x) variations relative to the lateral distance from the dike tip for each of the modeled layer arrangements and stiffness contrasts tested. The modeled dike is 4 km in length and its upper tip is located at a depth of 4 km. The line colors indicate the geometry of the layers from homogeneous (i.e., where the segment is one material) to horizontal and inclined at 10, 25 and 45 degrees. In A) the stiffness contrast between the layer hosting the dike (E_1) and the inclined layer (E_2) is 100:1, in B) 1:100, in C) 10:1 and in D) 1:10.

ADDITIONAL REFERENCES CITED

Amadei, B., and Stephansson, O., 1997, Rock stress and its measurement. (Chapman Hall, New York).

Druitt, T., Edwards, L., Mellors, R., Pyle, D., Sparks, R., Lanphere, M., Davis, M., and Barriero, B., 1999, Santorini Volcano. Geological Society Memoir 19:165.

Gudmundsson, A., 2011, Rock fractures in geological processes. Cambridge University Press. 578.

Gudmundsson, A., 2020, Volcanotectonics: Understanding the Structure, Deformation and Dynamics of Volcanoes. Cambridge: Cambridge University Press. doi:10.1017/9781139176217.

Heap, M.J., Villeneuve, M., Albino, F., Farquharson, J.I., Brothelande, E., Amelung, F., Got, J.L., and Baud, P., 2020, Towards more realistic values of elastic moduli for volcano modelling. Journal of Volcanology and Geothermal Research, 390, p.106684.

Rivano, S., Godoy, E., Vergara, M., and Villarroel, R., 1990, Redefinición de la Formación Farellones en la Cordillera de los Andes de Chile Central (32-34 S). *Andean Geology*, *17*(2), 205-214.